DRIVEN AND FREELY-DECAYING NONLINEAR SHAPE OSCILLATIONS OF DROPS AND BUBBLES IMMERSED IN A LIQUID: EXPERIMENTAL RESULTS

E.H. Trinh, D.B. Thiessen [1], and R.G. Holt [2]
Jet Propulsion Laboratory
California Institute of Technology

ABSTRACT

Large amplitude oscillations of drops and bubbles immersed in an immiscible liquid host have been investigated using ultrasonic radiation pressure techniques. Single levitated or trapped drops and bubbles with effective diameter between 0.4 and 0.8 cm have been driven into resonant shape oscillations of the first few orders. The direct coupling of driven drop shape oscillations between the axisymmetric $l=6$ and $l=3$ modes has been documented as well as the interaction between axisymmetric and non-axisymmetnc modes. Effective resonant coupling from higher to lower order modes has been observed together with a much less efficient energy transfer in the reverse direction. The first three resonant modes for bubbles trapped in water have also been excited, and mode coupling during driven and free-decaying oscillations has been measured. The evidence gathered thus far indicates that efficient drop resonant coupling from a higher to a lower order mode occurs when the characteristic frequency of the latter mode roughly coincides with a harmonic resonance.

[1] Department of Ph ysics, Washington State Universi ty
[2] Department of Mechanical Engineering, Boston University

1. INTRODUCTION

Single drop and bubble dynamics arc associated with multi-component and multi-phase dispersions occurring in nature and in industrial processes involving liquid-liquid extraction, distillation, or direct contact heat transfer. An improved understanding of the details of the often nonlinear interfaced dynamics should lead to a more accurate modeling of the relevant large-scale processes. In addition, a fundamental understanding of the dynamics will favorably impact the development of methods for the accurate determination of the physico-chemical properties controlling the motion of the drops and bubbles.

The levitation or trapping of single isolated fluid particles allows the control of their position, of their mechanical stimuli, and the accurate measurement of their response. By controlling the time variations of electric or acoustic force fields, contactless static and time-varying shape distortions can be induced and analyzed both in the transient as well as steady-state regimes. Practical interest in the deformation and shape oscillations of drops and bubbles immersed in liquid hosts arises because of their impact on particle size distribution in Iarge-scale fluid dispersion systems through fission and coalescence (Blass, 1990, Wright and Ramkrishna, 1994). The effects of shape deformation and oscillations on the efficiency of mass and heat transport have also been investigated in the past using translating **fluid particles in a liquid or gaseous host** (Kawalski and Ziolkowski, 1981, Kaji et al., 1980, Scott et al., 1990). The observed increase in the transport rates of oscillating drops cannot be attributed to the increase in surface area alone. Rather, the details of the dynamics of the shape oscillations and their impact on the fluid circulation around and inside the drops or bubbles are believed to play the pri mary role in this enhancement.

Because of inter-particle collision and flow perturbations, the shape deformations of individual droplets and bubbles in dispersions are often large, and the resulting shape osci llations are consequentl y nonl inear. Theories based on smal I amplitude approximations (Rayleigh 1879, Lamb 1881, Miller and Scriven 1968, Prosperetti 1980, Marston 1980) cannot accurately describe the details of the dynamics in this amplitude range. The fundamental characteristics of nonlinear in viscid drop shape oscillations have been addressed by Tsamopoulos and Brown (1984) through mu] tiple time-scale expansion and by Natarajan and Brown (1986) who derived the equations describing the nonlinear interaction of resonant modes by using the variational principle for the Lagrangian of the oscillatory motion. The quadratic and third order couplings of axisymmetric resonant modes of charged drops freely suspended in a tenuous medium (vacuum or gas) were

considered in the former study, and uncharged drops were treated by the latter authors. The principal predictions obtained were the quadratic decrease of the drop and bubble resonant mode frequencies as a function of the oscillation amplitude, and the resonant coupling of modes whose frequencies are integer multiples. Such modal interactions have been characterized by either aperiodic or periodic modulations of the amplitude and phase of the interacting modes. Experimental corroboration has been obtained for the amplitude dependence of the fundamental mode resonance frequency for drops suspended in liquid and in air, but no evidence for soft nonlinearity in the resonance frequency has yet been provided for the case of bubbles in liquids. Similarly, no experimental evidence for nonlinear modal coupling has yet been presented for drops and bubbles immersed in a liquid. In this paper, we will address some of these particular issues by presenting experimental observations of modal coupling of the resonant modes of both drops and bubbles immersed in a liquid host and driven into shape oscillation by the modulation of the ultrasonic radiation pressure.

2. EXPERIMENTAL APPROACH

In this work, we use a primary ultrasonic startding wave to support a drop or trap a bubble against gravity, and we modulate this wave at a vastly lower frequency to drive the drop into shape oscillations. A technique developed for previous experimental studies of linear and nonlinear drop (Marston and Apfel; 1979, Trinh, Zwern, and Wang; Trinh and Wang, 1982) and bubble shape oscillations (Asaki, Marston, and Trinh, 1993) has thus been used to gather the data reported in this paper. This particular implementation of the acoustic levitation method has thus been previousl y described in detail, and onl y a cursory discussion will be presented here. As shown in **figure 1** a liquid-filled cell with square cross section is excited into resonance through direct coupling to the piezo-electric transducer attached at its bottom. A specific three-dimensional ultrasonic standing wave in the liquid column is excited near the fundamental longitudinal (length) mode of the transducer (around 22.5 kHz) or at one of its odd harmonics (around 66 kHz). The empirical frequent y matching of these two resonances is carried out by varying the height of the liquid column, and a typical desirable resonant mode provides isolated three-dimensional acoustic pressure nodes and antinodes near the cell axis of symmetry. Liquid drops which are more compressible than the host liquid are driven toward and levitated near pressure antinodes (Apfel, 1976), and gas bubbles which arc smaller (larger) than resonant size arc driven toward and trapped near pressure antinodes (nodes) (Eller, 1968). The

bubble resonant size is that at which the volumetric bubble resonance frequency is equal to [hat of the standing wave. This volumetric mode frequency ω_R (the Minnacrt frequency) is approximately given by

$$\omega_R^2 = \left\{ \frac{3\gamma P_o}{\rho R^2} - \frac{2\sigma}{\rho R^3} \right\} \qquad (1),$$

where y is the ratio of the specific heats of the gas, P. is the ambient hydrostatic pressure, σ the surface tension, ρ is the liquid density and R the equilibrium bubble radius. For the bubble sizes of interest in this study, the second term on the right side is small compared to the first term.

In this paper we report results obtained with both drops and bubbles, the latter always larger than critical size, and trapped slightly above a local pressure node. An experimental study of the large amplitude oscillations of drops levitated in air and under the combined action of electric and ultrasonic fields has been reported elsewhere (Trinh, HoIt, Thiessen, 1996).

Modulation of the acoustic radiation stresses acting on the interface has provided the drive for the shape oscillations. This was primarily carried out through direct modulation of the fundamental levitation standing wave, but the amplitude modulation of the third harmonic has also been implemented in order to provide a greater stress on the individual fluid particles. For the amplitude modulation of the radiation pressure, the voltage across the ultrasonic transducer, V_{ac} , is given by

$$v_{ac} = v_{ac0}[1+ M\cos(\omega_m t)]\cos(\omega_{ac} t), \qquad (2)$$

v_{ac0} is the amplitude of the carrier voltage at the frequency $\omega_{ac} = 2\pi f_{ac}$ for the acoustic standing wave (f_{ac}=22.5 kHz), M is the modulation index for the amplitude modulation of the acoustic force at the frequency ω_m. Because the acoustic radiation force is proportional to the square of the acoustic pressure, this force is therefore proportional to V^2_{ac} , and this amplitude modulation results in a time-varying acoustic force at both the frequencies ω_m as well as $2\omega_m$. This results in a *periodic flattening of the drop or bubble by the acoustic force* when the fluid particle diameter is small compared with the ultrasonic wavelength. When the particle diameter is a significant fraction of the ultrasonic wavelength, however, the periodic elongation of the drop or bubble along the vertical axis can also be obtained

through amplitude modulation of the acoustic pressure. A static distortion of the drop or bubble can also be induced by the ultrasonic levitation or trapping field as the size of the fluid particle becomes a non-negligible fraction of the wavelength. **Figure 2a** shows the unmodulated shape of a large air bubble of approximately 0.8 cm in diameter and trapped in a 22.9 kHz sound field. In addition to the shape asymmetry with respect to the equator, one can also notice the presence of short-wavelength capillary waves on the upper hemisphere of the trapped bubble. **Figure 2 b is** a magnified image obtained under short duration stroboscopic illumination and shows the capillary waves in greater detail. The frequency of these waves have been determined to be around 11 kHz, indicating that the generating mechanism is probably through the Faraday instability (Holt and Trinh, 1994). The latter has also been shown to induce resonant shape oscillations for smaller bubbles (20 to 30 μm in diameter) which are initially acoustically driven in the radial mode (Holt and Gaitan, 1996). The presence of these capillary waves and the fact that the equilibrium shape of the trapped bubbles is not spherical both influence the characteristics of the shape oscillations. The details of such effects are beyond the scope of this paper, however, but they will be addressed in a forthcoming low-gravity investigation to be carried out using a similar experimental apparatus.

An acoustically-induced steady-state convective flow field is also present in the liquid outside of the trapped bubble as shown in **figure 3.** This time-exposure photograph of both a trapped bubble and its immediate surrounding shows steady and oscillatory circulation both inside and outside of the bubble (in the air and in the liquid). The outer streaming in the liquid has been documented previously and is expected, but the inner flow has not been seen before and is under more detailed scrutiny. The results will be reported in a later publication.

The driven and freely-decaying shape oscillations of both drops and bubbles were monitored by standard (30 frames/second) and high-speed (2,000 frames/second) video cameras. To facilitate the automated analysis of the drop or bubble shapes from the digitized individual video frames, backlighting was selected as the primary illumination technique. The high-contrast, dark contours in a bright background were analyzed with an edge-finding routine, and the experimental data were fitted into axisymmetric shapes with the usual expansion in terms of the time-dependent surface spherical harmonics.
The shape of the drop or bubble, described by $R(\theta, t)$ is expanded as

$$R(\theta, t) = R_0 \left[1 + \sum_{l=2}^{l^*} \left[c_l(t) P_l(\cos\theta) \right] \right], \qquad (3)$$

where R_0 is the radius of the sphere of the same volume, $P_l(\cos\theta)$ is the Legendre polynomial of degree l, and $c_l(t)$ are the corresponding coefficients. Using this method we can obtain the time series for each cl(t) for driven and freely decaying shape oscillations. For the data described in this paper, wc have limited ourselves to $l^*=6$. A digitally analyzed video frame up to a maximum of 320 x 240 pixels and in 256 levels of gray. **Figure 4** shows a series of shapes recorded on still video for a drop initially driven into the axisymmetric 1=3 mode and subsequently exciting the non-axisymmetric l=2 mode. This case is discussed in a later section of this paper. **Figure 5** shows the photographs of the extremum shapes of a drop initially driven into the l=6 mode and subsequently exciting the l=3 rode. This case is also discussed in the following section. The illumination used for the drop photographs is a combination of back and side lighting.

3. EXPERIMENTAL RESULTS

Drop Shape Oscillations

The first few *driven* resonant shape oscillations of drops immersed in a liquid host have been previously observed by using ultrasonic radiation pressure (Marston and Apfel, 1979; Trinh, Zwern, and Wang, 1982; Annamalai and Trinh, 198S) and electric field drive (Rhim, Elleman, and Saffren, 1982; Scott, Basaran, and Byers, 1990; Azuma, Yoshihara, and Ohnishi, 1989). Although the controlled excitation and measurement of the well resolved and independent resonant modes and the experimental evaluation of the weak nonlinear characteristics of the fundamental quadrupole (oblate-prolate) mode has allowed the validation of both the linear theory as well as predictions from nonlinear numerical calculations (Tsamopoulos and Brown, 1984), no data on resonant mode *coupling* has yet been published. In this paper wc report the observations of the interaction between resonant modes when their nominal resonant frequencies satisfy an approximate integer multiple relationship. The strongest coupling has been found for a 2:1 ratio where a mode is initially acoustically driven at high amplitude, and a lower order mode is subsequently and excited at a sub-harmonic frequency due to nonlinear interaction.

The materials used for these studies are silicone oil (Polydimethylsiloxanes) with a kinematic viscosity of 2 cSt for the drops and distilled outgassed water for the host liquid. The drop diameter ranged from 1.0 to 1.5 cm, and the ultrasonic frequencies of the standing waves used to excite the shape oscillations were 22.5 and 66 kHz.

COUPLING BETWEEN THE L=3 AND L=2 MODES

Figure 6 summarizes the experimental results for a 1.1 cm diameter silicone oil drop in water. The drop videotape frames capturing the drop motion were digitized and the drop contour on each frame was continuously fitted with 100 points. Assuming axial symmetry, this drop boundary was decomposed into shapes associated with Legendre polynomials. These coefficients (between C_2 and c_6) are plotted in **figure 6a.** The volume is calculated *assuming axial symmetry*, and is also plotted in order to check the constant volume restriction.

In this particular measurement, the drop was initially driven in the l=3 axisymmetric mode resonance (at 2.15 Hz) at large amplitude (20% of the drop diameter). The steady-state oscillations are characteristically tit-cc-lobed and they can be viewed along a horizontal view axis (see **figure** 4), while an oscillating circular cross section can be seen along the orthogonal vertical axis (symmetry axis). This is confirmed by the plot of the volume which shows a constant value centered at 1.0. At about 150 frames, the amplitude of the l=2 mode Legendre coefficient (c_2) begins to increase, and displays a sub-harmonic time-dependence at 1.07 Hz. These l=2 mode *oscillations* grow in amplitude at the expense of the l=3 oscillations, but they are *not* axisymmetric along the vertical axis. Rather, they are aligned along a horizontal direction normal to the symmetry axis. This is reflected by the deviation of the calculated volume from unity. The acoustic shape oscillation drive is removed after 360 frames, and the decay of all the shape oscillation modes can be observed.

One might note that according to linear theory results (Marston, 1980), the ratio of the small amplitude resonance frequencies ω_3 / ω_2 is near 1.S2 for the current conditions and for axisymmetric modes. The lower frequency value (factor of 2) corresponding to the sub-harmonic frequency drive observed here, could be explained by soft nonlinearity in large amplitude drop shape oscillations (Trinh, Wang, 1982), detuning duc to viscous effects, or it might cw-respond to a lower resonance frequency for the non-axisymmetric mode which has been excited in this particular case. We have observed the removal of the

degeneracy for these resonant oscillations (three different l=2 modes can be driven at slightly different frequencies grouped around the theoretically predicted resonance). An anal ysis of the removal of the degeneracy by a static shape deformation is also avai lable in the literature (Suryanarayana and Bayazitoglu, 1991). In previously reported experimental results on drops levitated in air (Trinh, HoIt, and Thiessen, 19%), three separate l=2 modes were also observed, and a ***non-axisymmetric mode was found to have the lowest frequency.*** If the same is true for this case, the frequency ratio of the axisymmetric l=3 mode to the non-axisymmetric l=2 mode would be closer to 2.

In **figure** 6 **b are plots** of Fourier transforms of the time-dependent Legendre coefficients, and show the frequency spectrum for each of the Legendre shape. The Fourier transforms were calculated using all the data shown in the time dependence plots. The first obvious characteristic is the presence of the initial *driven* frequency 2.15 Hz of the l=3 mode on ***all*** of the spectra for the corresponding Legendre coefficients. This indicates that large amplitude oscillations in an initially pure mode will drive motion which has other characteristic higher order mode shapes all having the same *initial driven frequency.* This was predicted by Feng and Beard (1990,1991) when they considered the case of electrically driven oscillations of charged drops in a gas. Interestingly, the sub-harmonic frequency strongly appears only in the 1=2 and somewhat weakly in the l=5 mode spectra. Another salient characteristic is the excitation of a near second harmonic component at 4.2 Hz corresponding to the l=5 mode oscillations. The l=5 mode linear resonance frequency is roughly twice that of the l=3 mode.

Also significant is the fact that we have not been able to get a strong coupling in the reverse direction, i.e. it has not been possible to drive the l=3 *mode at its characteristic resonance frequency* by acoustically exciting the axisymmetric or nonaxisymmetric l=2 oscillations. Large amplitude driven l=2 motion generates 1=3,4,5,6 shapes at its driven frequency as well as its harmonics. For example, the l=3 oscillatory shapes have the frequency of the driven l=2 mode, and l=4 oscillations arc found to have frequency components at f(l=2) and at 2xf(l=2) instead of 3xf(l=2) as prescribed by linear theory. This appears to agree with previously published results based on a nonlinear analysis of the decay of drops released from a nozzle (Becker, Hiller, and Kowalewski, 1994).

These results can be summarized as follows: (l) Large-arnplitudc acoustically driven resonant oscillations in a pure mode can *sub-harmonically* excitc a corresponding resonant mode having different symmetry characteristics, (2) They generatc the first fcw of

the Legendre axisymmetric shapes at the *same driving frequency,* and (3) They can also drive *higher harmonic* resonant mode osci nations (second harmonic in this case) as predicted by Tsamopoulos and Brown (1984).

COUPLING BETWEEN THE L=6 AND L=3 MODES

In this second case, a 1.5 cm diameter silicone oil drop was levitated in distilled water and driven into resonant l=6 mode oscillations (see **figure 5), Figure 7a** shows the initial driven motion of the c_6 Legendre coefficient at 6.7 Hz, the rising amplitude of the C_3 coefficient, and the steady driven 1=3 oscillations at the sub-harmonic frequency of 3.4 Hz. A slight non-axisymmetric component at the same sub-harmonic frequency is detected in the plot of the calculated volume as a function of time. Also observable is the rising importance of the sub-harmonic frequency in the time dependence of both the c_2 and C_4 coefficients. **Figure 7 b,** showing the plots of the Fourier transform of the Legendre coefficients, confirms the presence of the driving and sub-harmonic frequency. The second harmonic frequency component is not apparent in this case because the resonant mode response at such a high frequency (13.4 Hz) is highly damped by viscosity.

Onc must note, however, that the calculated small-amplitude normal mode frequency ratio ω_6 / ω_3 is approximately equal to 2.5, not 2.0. In this case the sub-harmonic frequency appears higher than the small-amplitude resonance frequency of the secondary (non-lined y driven) mode. Thus, there appears to be a significant degree of detuning in the sub-harmonic drive of the l=3 characteristic mode. This is not surprising due to the increased viscous damping associated with the higher order mode. In addition, because of the soft nonlinearity of large amplitude shape oscillations, the actual resonance frequency of the l=6 mode is shifted to a lower value than predicted by the linear theory. The actual frequency ratio could therefore be smaller than 2.5 by as much as 15% when previous experimental results and theoretical predictions are taken into account (Tsamopoulos and Brown, 1983; Tnnh and Wang, 1982).

COUPLING BETWEEN THE L=4 AND THE L=2 MODES

In this third case, a 1.2 cm diameter silicone oil drop in distilled water was initially driven into resonant l=4 axisymmetric oscillations (scc the c4 coefficient plotted as a

function of time in figure 8). The fairly large amplitude driven oscillations in the l=4 mode appear to excite even numbered oscillations (l=2 and l=6) at the same frequency, but they do not appreciably induce odd-numbered mode motion (l=3 and l=5). This is in agreement with predicted behavior (Tsamopoulos and Brown, 1984, Feng and Beard, 1990). The time-dependence of the l=2 mode motion is a superposition of two frequencies: the natural, lower, resonance frequency of the quadruple oscillations and the driving frequency of the l=4 mode. Also note that the l=2 mode oscillations are about a substantially oblate equilibrium configuration (the value of the c2 coefficient is negative throughout the shape oscillations).

According to linear theory for spherical drops, the ratio of the l=4 to 1=2 mode frequencies is about 2.6. The actual frequency ratio for large amplitude oscillations will be lower for the same reasons mentioned in the preceding case. In addition, the equilibrium shape of the drop under study is not spherical and its resonance frequencies would also be shifted to values lower than predicted by linear theory (Trinh, HoIt, and Thiessen, 1996; Shi and Apfel, 1995). Thus, harmonic resonance still appears to be a reasonable interpretation.

Bubble Shape Oscillations

Shape oscillations have been experimentally observed in the past in the context of the shape stability of radian y oscillating small bubbles: as the amplitude of the volume oscillations of bubbles trapped in an ultrasonic standing wave increases, resonant surface standing waves (shape oscillations) are parametrically excited through the Faraday instability mechanism (Strasberg and Benjamin, 1958; Eller and Crum, 1970). Other workers have also driven these shape modes directly by *mechanically restraining* bubbles in a wire loop and exciting an acoustic traveling wave in the kiloHertz frequency range (Francescutto and Nabergoj, 1978). Recent advances in the technique for ultrasonically trapping larger, millimeter-size bubbles have permitted the detailed analysis of certain aspects of the damping of their shape oscillatory dynamics (Asaki, Marston, Trinh, 1993, Asaki, Thiessen, and Marston, 1995). In this particular paper, we report some quantitative measurements of the characteristics of large amplitude shape osci nations of air bubbles several millimeters in diameter and trapped in distilled water.

SHAPE OSCILLATIONS OF AIR BUBBLES ACOUSTICALLY TRAPPED IN WATER

Air bubbles trapped by the 22.5 kHz standing wave were initially driven in one of the resonant shape modes and the subsequent freely decaying oscillations were analyzed using modal decomposition in the same manner as described in previous sections for the case of drops. The initial oscillation amplitude was generally on the order of, or larger than 10% of the equivalent equilibrium bubble radius. Our attention was mainly focused on the excitation of neighboring resonant modes. The experimental time resolution for all the data sets presented below was 1 millisecond.

Figure 9 shows plots of the first five Legendre coefficients and of the volume as a function of time for a 0.42 cm diameter air bubble initially driven into the axisymmetric l=2 resonant mode (49.5 Hz). The most notable higher mode excitation at the appropriate *characteristic resonance* frequency is revealed by the response of the 1=3 mode. Dual frequency response is detected during both the driven and free-decay phases: both the driving frequency as well as roughly double that frequency are clearly visible in the C3 time response curve. The evidence also shows that the l=4, and to a much smaller extent the l=5 and l=6 shapes, were also driven at the *same l=2* frequency during the acoustically-driven phase.

Figure 10a displays plots of the Legendre coefficients as a function of time for a 0.41 cm diameter air bubble initially driven into the axisymmetric l=3 mode (83 Hz). As shown before, all the resonant shapes are excited at the single driving frequency in the steady-state regime. A characteristic nearly single frequency decay is measured for the l=2 mode as soon as the acoustic drive is terminated, while both the l=3 and l=4 modes display a superposition of the l=2 and of their characteristic normal mode free-decay frequencies. This is better shown in **Figure 10b** where the Fourier transform of the time-series data in the *free-decay region* was performed. The lowest order (l=2) and the next higher (l=4) modes frequencies are not harmonically related to the excitation frequency, the experimental results for the mode frequency ratios arc f(l=3) / f(2) = 1.71 and f(l=4) / f(l=2) = 2.43. These values are lower than the linear theoretical values for ideal spherical drops of 1.82 and 2.56 respectively.

Figure 11 reports similar results except that the initial acoustic drive was for the l=4 mode (136.5 Hz). Once again, the l=2 natural free-decay frequency is present in all the Legendre coefficient time series, and each characteristic mode frequency is generated in the

free-decay phase. The freely decaying oscillations of the higher modes arc thus modulated by the least damped natural oscillations in the fundamental quadrupole mode.

4. DISCUSSION and SUMMARY

Driven large amplitude shape oscillations responses of drops and freely decaying oscillations of bubbles have been investigated in this work. Ample evidence for sub-harmonically and harmonically-induced mode coupling has been documented for both drops and bubbles. This is at least in partial agreement with the theoretical predictions of Tsamopoulos and Brown (1984).

For drops, the more significant result described here is the uncovering of an efficient sub-harmonic excitation of a resonant mode concurrent with the usual higher harmonic excitation. The former is more efficient due to the increasingly greater viscous damping of shape oscillations with higher mode numbers. A certain degree of detuning has also been found to be acceptable for subharmonic excitation: exact matching of the natural resonance frequency of this secondary mode to half the drive frequency is not required. Also significant is the fact that a mode of different symmetry characteristics can be excited as long as its resonance frequency is close to half the drive frequency. Finally, all shape oscillation modes are driven at the excitation frequency, and it appears that even-numbered modes do not easily couple to odd-numbered ones, while odd-numbered modes can excite even modes. This is in agreement with previous theoretical work describing the dynamics of electrostaticall y levitated charged drops (Tsamopoulos and Brown, 1984; Feng and Beard, 1990 and 1991).

In the case of bubbles, it is clear that the free-decay dynamics are dominated by the least damped mode, regardless of the nature of original driven mode. As in the case for drops, all the modes are driven at the excitation frequency, but the bubbles higher order modes are found to freely decay at their characteristic resonant frequency superposed on the fundamental mode frequency. The deformed, semi-oblate shape of these trapped bubbles is not symmetrical with respect to the equator. This non-spherical equi Ii brium shape could explain why the experimental ratios for the resonant mode frequencies are lower than the predictions from linear theory.

Because of the need for levitation (or trapping) the fluid particles arc not totally free. This is reflected in the oblate equilibrium shapes of the relatively large air bubbles studied

here and in the outer liquid streaming flows. The drops and bubbles are thus not completely free of external influence since they arc constrained to remain at a fixed location by the sound field. It has been theorized that the equilibrium shape of the drop or bubble also plays a significant role in *the* mode coupling processes involved at large amplitude oscillations. This may be intuitive y understood once the shifting of the resonance frequencies by static shape deformation and removal of mode degeneracy is taken into account. The performance of the same experiments in low gravity where all positioning forces are turned off during the free-decay phase would provide results devoid of field interference, and it might provide a direct quantitative assessment of this bias.

Previous theoretical works dealing with weakly viscous drops have suggested a significant influence of viscosity on nonlinear mode coupling characteristics (Basaran, 1992; Becker, Hiller, and Kowalewski, 1993). The results reported here point to an obvious bias toward the secondary excitation of less damped and harmonically-related resonant modes during the active excitation of a primary mode at large amplitude. The apparent significant degree of detuning observed here also suggests the influence of viscous effects, although this may also emphasize the effect of the soft nonlinearity in the resonance frequencies.

ACKNOWLEDGMENTS

This work was carried out at the Jet Propulsion Laboratory, California Institute of Technology under contract with the Microgravity Research Division of the National Aeronautics and Space Administration. We also thank the referees for many helpful and insightful suggestions.

REFERENCES

Annamalai, P., Trinh, E., and Wang, T.G. 1985 Experimental study of the oscillations of a rotating drop, J. Fluid Mech. **158,** 317-327.

Apfel, R. E., 1976 Technique for measuring the adiabatic compressibility, density, and sound speed of submicroliter liquid samples, J. Acoust. Sot. Am. 59, 339.

Asaki, T. J., Marston, P. L., and Trinh, E.H. 1993 Shape oscillations of bubbles in water driven by modulated ultrasonic radiation pressure: Observations and detection with scattered laser light, J. Acoust. Sot. Am., 93, 706-713.

Asaki, T. J., Thiessen, D. B., and Marston, P. L., 1995 Effects of an insoluble surfactant on capillary oscillations of bubbles in water: observation of a maximum in clamping, Phys. Rev. Lett. 7 S, 2686-2689.

Azuma, H., Yoshihara, S., and Ohnishi, M., 1989 An experimental study of electricall y excited liquid-drop oscillations, 40th Congress of the International Astronautical Federation, IAF-89-448.

Becker, E., Hiller, W. J., and Kowalewski, T.A. 1994, Nonlinear dynamics of viscous droplets, J. Fluid Mech. 258, 191-216,

Blass, E. 1990 Formation and coalescence of bubbles and droplets. Int. Chem. Eng. 30, 206-221.

Eller, A.I. 1%8, Force on a bubble in a standing acoustic wave, J. Acoust. Sot. Am. 43, 170-171 (L).

Eller, A. and Crum, L.A. 1970 Instability of the motion of a pulsating bubble in a sound field, J. Acoust. Soc. Am. 47, 762.

Feng, J.Q. and Beard, K.V. 1990 Small amplitude oscillations of electrostatically levitated drops, Proc. Roy. Sot. London Ser. A 430, 133 ; 1991 Three-dimensional oscillation characteristics of electrostaticall y deformed drops, J. Fluid Mech. 227, 429.

Francescutto A. and Nabcrgoj, R. 1978 Pulsation amplitude threshold for surface waves *on oscillating* bubbles, Acustica, 41,215-220.

HoIt, R.G. and Gaitan, D.F. 1996, Observation of stability boundaries in the parameter space of single bubble sonoluminescence, Phys. Rev. Lett. 77, 3791-3797.

Holt, R.G. and Trinh, E.H. 1994 Radiation pressure induced capillary waves, J. Acoust. Sot. Am. 95, Pt.2 2988 (A)

Kaji, N., Mori, Y. H., Tochitani, Y., and Komotori, K. 1985 Heat transfer enhancement due to electrically-induced resonant oscillation of drops. ASME J. Heat Transfer 107, 788-792.

Kawalski, W. and Ziolkowski, Z. 1981 Increase in rate of mass transfer in extraction columns by means of an electric field. Int. Chem. Eng. 21, 323-335.

Lamb, H. 1881 On the oscillations of a viscous spheroid. Proc. Lend. Math. Soc. 13, 51-56.

Marston, P. L. 1980 Shape oscillations and static deformation of drops and bubbles driven by modulated radiation stresses-Theory. J. Acoust. Sot. Am. 67, 15-26.

Marston, P. L. and Apfel, R. E. 1979 Acoustical y forced shape oscillation of Hydrocarbon drops levitated in water. J. CoIl. Interface Sci. 68, 280-286.

Miller, C.A. and Scriven, L.E. 1968 The oscillations of a fluid droplet immersed in another fluid. J. Fluid Mech. 32, 417-435.

Natarajan, R. and Brown, R. A. Quadratic resonance in the three-dimensional oscillations of inviscid drops with surface tension 186, Phys. Fluids 29, 2788-2797.

Prosperetti, A. 1980 Normal mode analysis for the oscillations of a viscous liquid drop immersed in another liquid. J. Méc. **19,** 149-182.

Rayleigh, Lord 1879 On the capillary phenomena of jets. Proc. R. Sot. Lend. 29,71-97.

Rhim, W. K., Elleman, D. D., and Saffren M. Normal modes of a compound drop. Proceedings of the Second International Colloquium on Drops and Bubbles, Monterey, CA Nov. 1981, NASA-JPL publication 82-7, 7-14.

Scott, T. C., Basaran, O. A., and B yers C.H. 1990 Characteristics of electric-field-induced oscillations of translating liquid droplets. Ind. Eng. Chem. Res. 29, 901-909.

Shi, T. and Apfel, R. E., 1995 Oscillation of a deformed liquid drop in an acoustic field, Phys. Fluids 7, 1545-1552.

Strasberg, M and Benjamin, T.B. 1958 Excitation of the oscillations in the shape of pulsating gas bubbles: experimental work (abstract) J. Acoust. Sot. Am. 30, 697.

Trinh, E, Zwern, A., and Wang T.G. 1982 An experimental study of small-amplitude drop oscillations in immiscible liquid systems. J. Fluid Mech. **115,** 453-474.

Trinh, E, Holt, R. G., and Thiessen, D. B., 1996 The dynamics of ultrasonically levitated drops in an electric field, Phys. Fluids. 6,3567-3579.

Tsamopoulos, J.A and Brown R.A. 1984 Resonant oscillations of inviscid charged drops J. Fluid Mech. **147,** 373-395.

Tsamopoulos, J.A. and Brown, R.A. 1983 Nonlinear oscillations of inviscid drops and bubbles, J. Fluid Mech. **127,** 519-537.

Wright, H. and Ramkrishna, D. 1994 Factors affecting coalescence frequency of droplets in a stirred liquid-liquid dispersion. AIChE J. 40,767-776.

FIGURE CAPTIONS

Figure 1:

Schematic description of the experimental apparatus. A Lucite square cross-section cavity has been machined to allow the mounting of a resonant piezoelectric transducer at the bottom of the chamber. This transducer is driven by a function generator and amplifier in order to establish a three-dimensional standing wave in the water filled chamber. This standing wave is amplitude modulated in order to modulate the acoustic radiation pressure to drive the levitated drops and trapped bubbles into shape oscillations. The data described in this paper has been acquired through the analysis of digitized frames from a high speed video camera recording the dynamics of the backlight fluid particles.

Figure 2:

a: Backlit image of a trapped 4.5 mm diameter air bubble in water. The structure faintly seen at the north pole are high frequency capillary waves excited through the Faraday instability on the air-water interface.

b: Higher resolution video frame of the capillary waves at the bubble north pole. The waves have been recorded with a video camera with high intensity-short duration pulsed lighting.

Figure 3:

Single video frames displaying the light scattered from a trapped air bubble containing suspended tracer particles. A steady-state streaming flow can be observed within the air bubble. The velocity distribution is highly non-uniform because the principal driving mechanism for streaming appears to be the capillary waves at the bubble top surface.

Figure 4:

Series of video single frames of a silicone oil drop in water initially driven into the axisymmetric 1=3 mode. Non-axisymmetric l=2 oscillations are gradually excited through harmonic resonance. The initial axisymmetric three-lobed oscillations are coupled with oblate-prolate shapes as shown on this view perpendicular to the original axis of symmetry. The series of five pictures on the left depicts axisymmetric l=3 mode shapes. The series of ten pictures on the right shows shapes of superposed l=3 and l=2 oscillations.

Figure 5:

Series of video single frames showing the shapes of an initially axisymmetric l=6 (on the left) and the shapes of the superposed l=6 and l=3 shape modes (on the right). The l=3 secondary oscillations arc excited by the large amplitude acoustically-driven l=6 mode. Characteristic three-lobed configurations arc seen superposed on the original six-lobed geometry.

Figure 6:

a.: Time dependence of the first five Legendre coefficients of a 1.1 cm diameter silicone oil drop levitated in water and initially driven into the axisymmetric L=3 resonant mode of shape oscillations. The sub-harmonic excitation of a non-axisymmetric L=2 resonant mode is the salient characteristic. A strong harmonic component can also be detected in the C4, C5, and C6 Legendre coefficient.

b: Fourier spectrum of the times series shown in a. Both sub-harmonic and harmonic components arc prominently displayed. All the data points shown in the time series have been used in the Fourier transform operation.

Figure 7:

a: Time dependence of the first five Legendre coefficients for a 1.5 cm diameter silicone oil drop levitated in water and initially driven into the L=6 resonant mode of shape oscillations. The sub-harmonic coupling leads to the *excitation* of the resonant L=3 mode accompanied by a very slight decrease in the amplitude of the response in the L=6 *mode.*

b: Fourier transforms of the data in a. prominently display that sub-resonant coupling. All the data points shown in the time series have been used in the Fourier transform operation.

Figure 8:

Time dependence of the Legendre coefficients for a 1.2 cm diameter silicone oil drop levitated in water and initially driven into the L=4 resonant mode of shape oscillations. Sub-resonant excitation drives the L=2 mode which responds at a combination of the driving and sub-harmonic frequencies.

Figure 9:

Time dependence of the Legendre coefficients for a 0.42 em diameter air bubble trapped in water. The bubble is initially driven into the L=2 mode and the oscillations are allowed to freely decay. Harmonics of the driving frequency can be detected, but an obvious characteristic is the presence of the driving frequency in the response of all the Legendre modes.

Figure 10:

Time dependence of the Legendre coefficients and FFT for a 0.41 cm diameter air bubble trapped in water and initially driven into its L=3 resonant mode. All the modes respond at the forcing frequency during the driven phase, but the characteristic frequencies of the normal modes are recovered during the free-decay phase, although they are modulated by the least-damped L=2 mode oscillations.

Figure 11:

Time dependence of the Legendre coefficients for an air bubble driven in its L=4 resonant mode. All modal responses arc at the driving frequency in the initial phase, but the characteristic modal frequencies are again recovered in the free-decay portion.

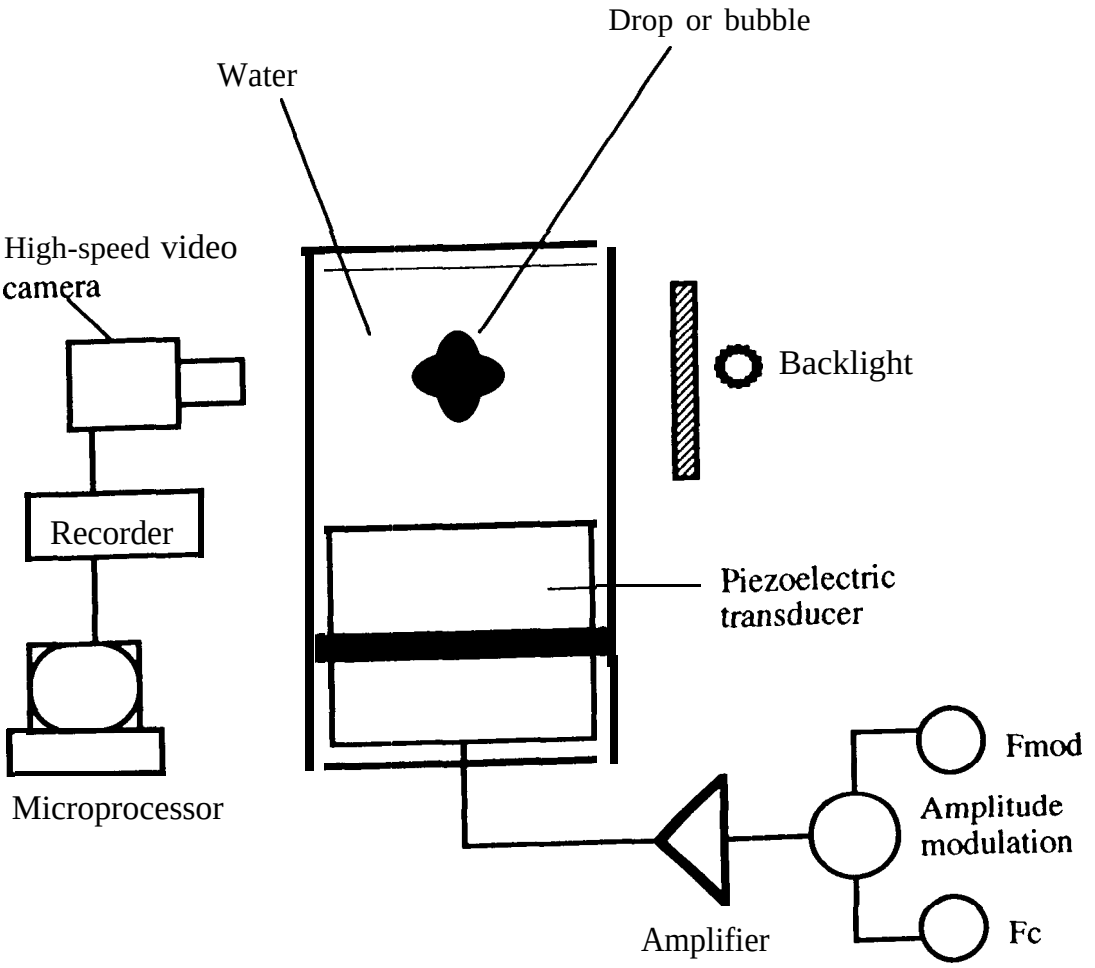
Drop or bubble
Water
High-speed video camera
Backlight
Recorder
Piezoelectric transducer
Microprocessor
Fmod
Amplitude modulation
Fc
Amplifier

Fig. 1

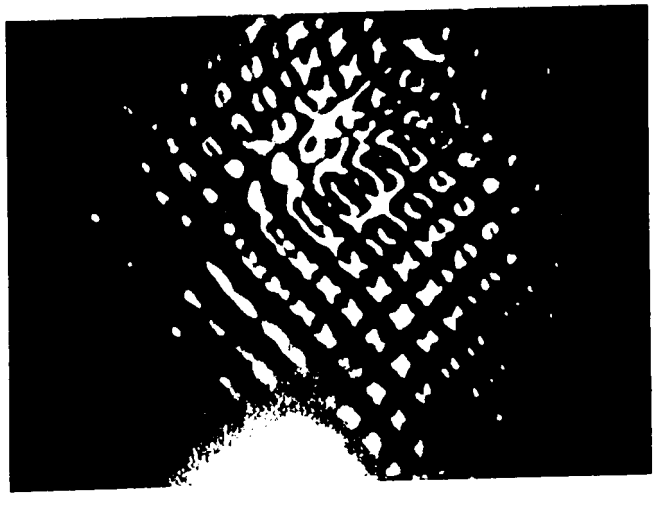

Fig. 2

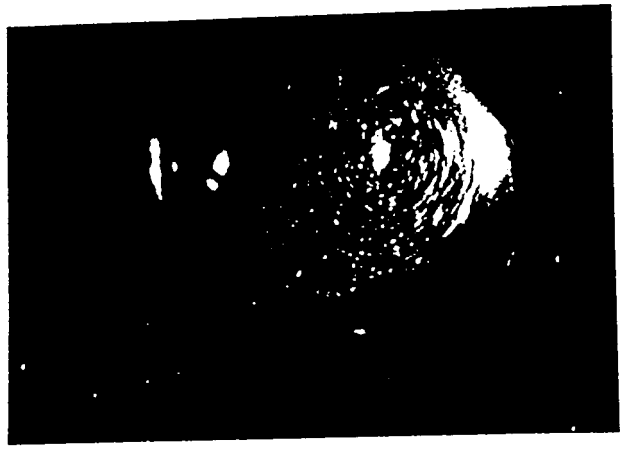

Fig. 3

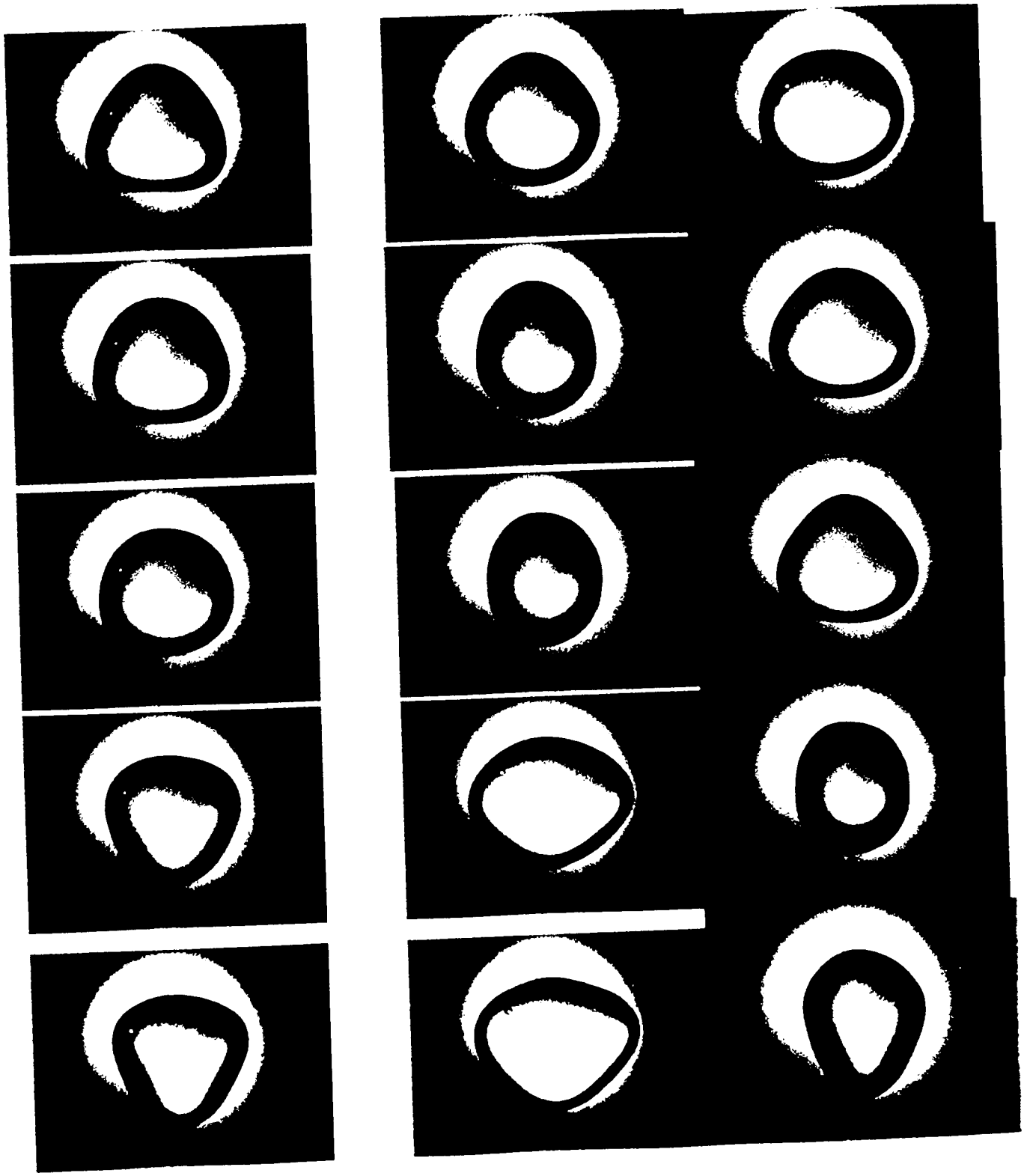

Fig. 1

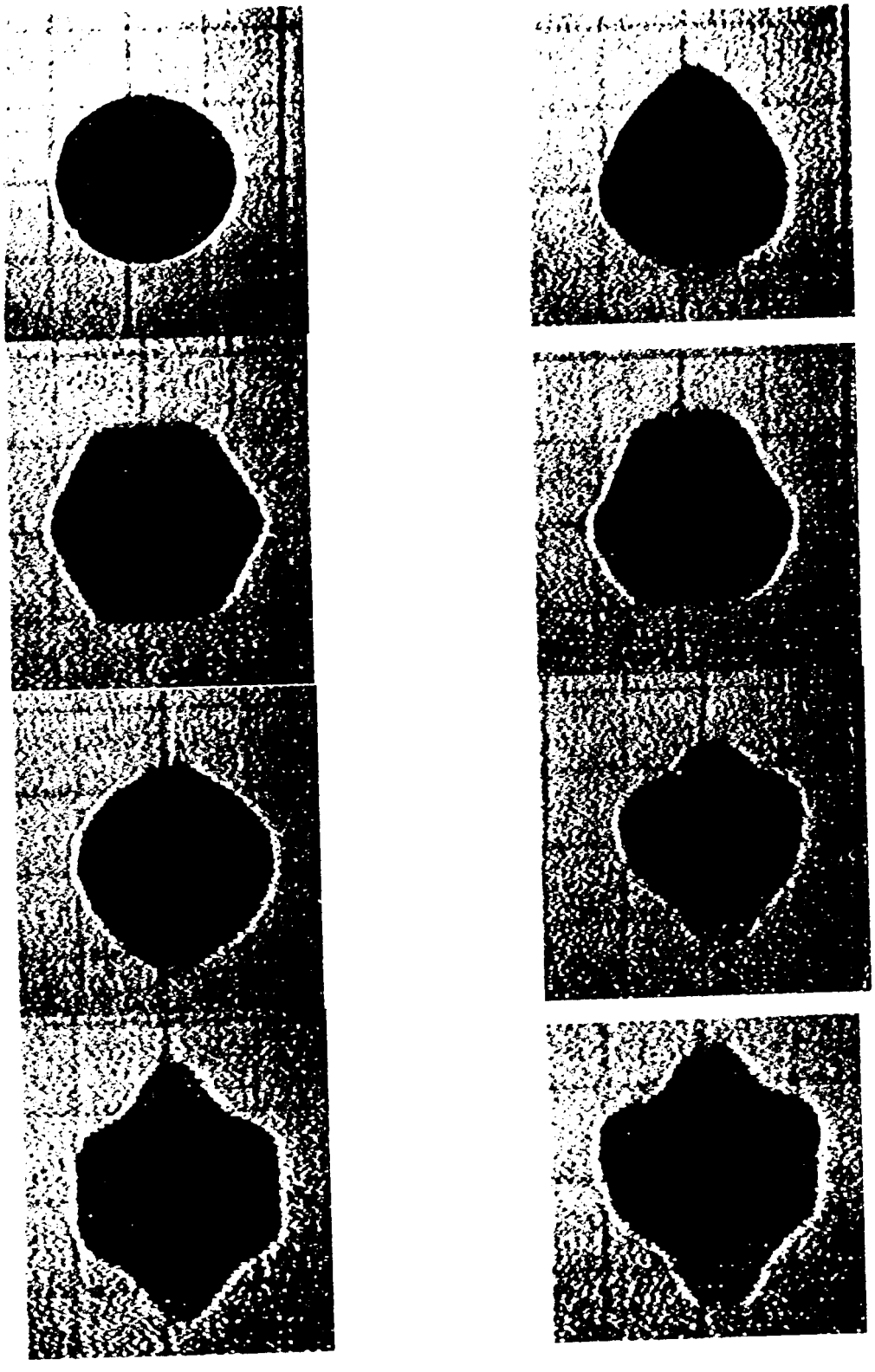

Fig. 5

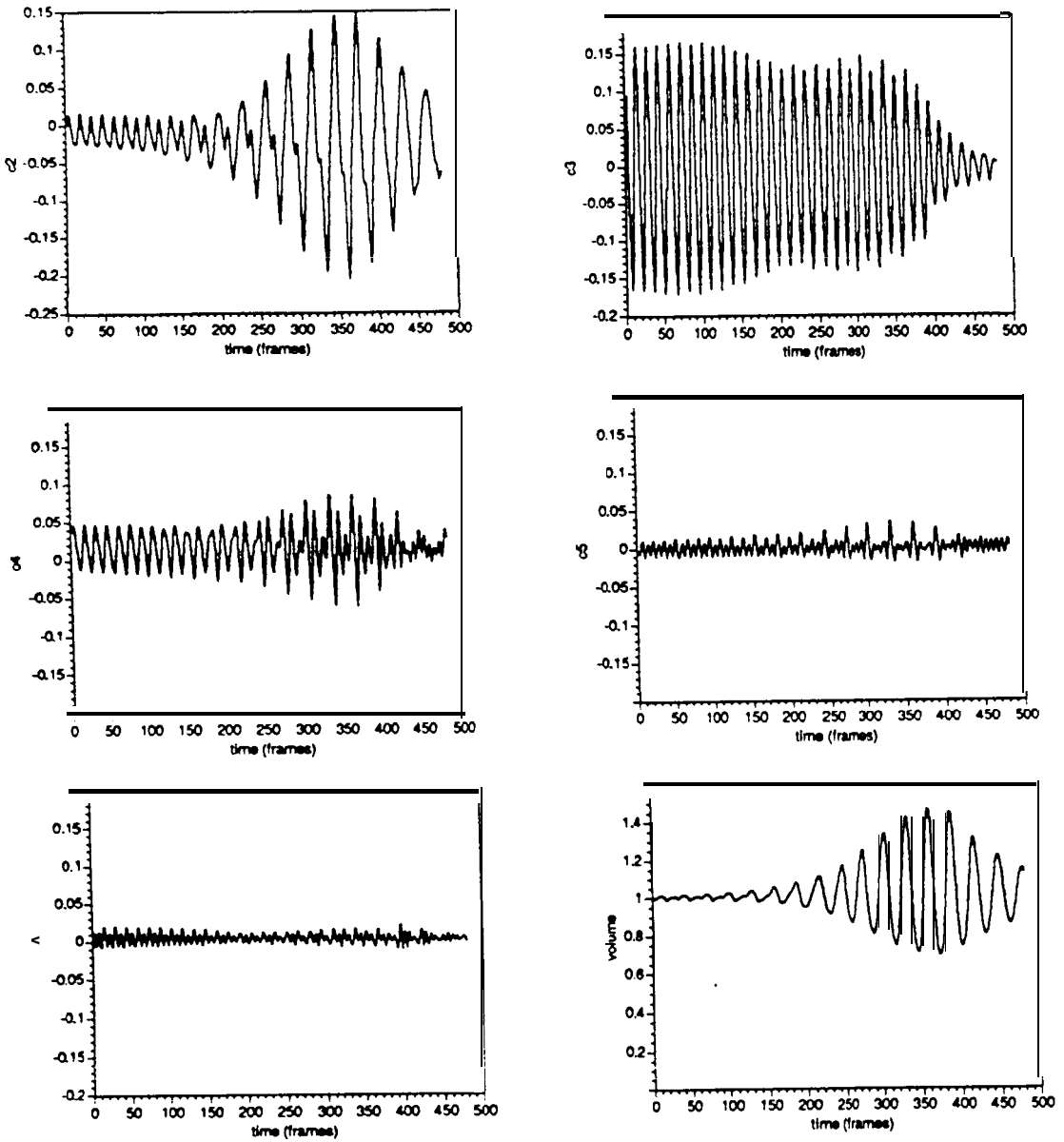

Fig. 6a

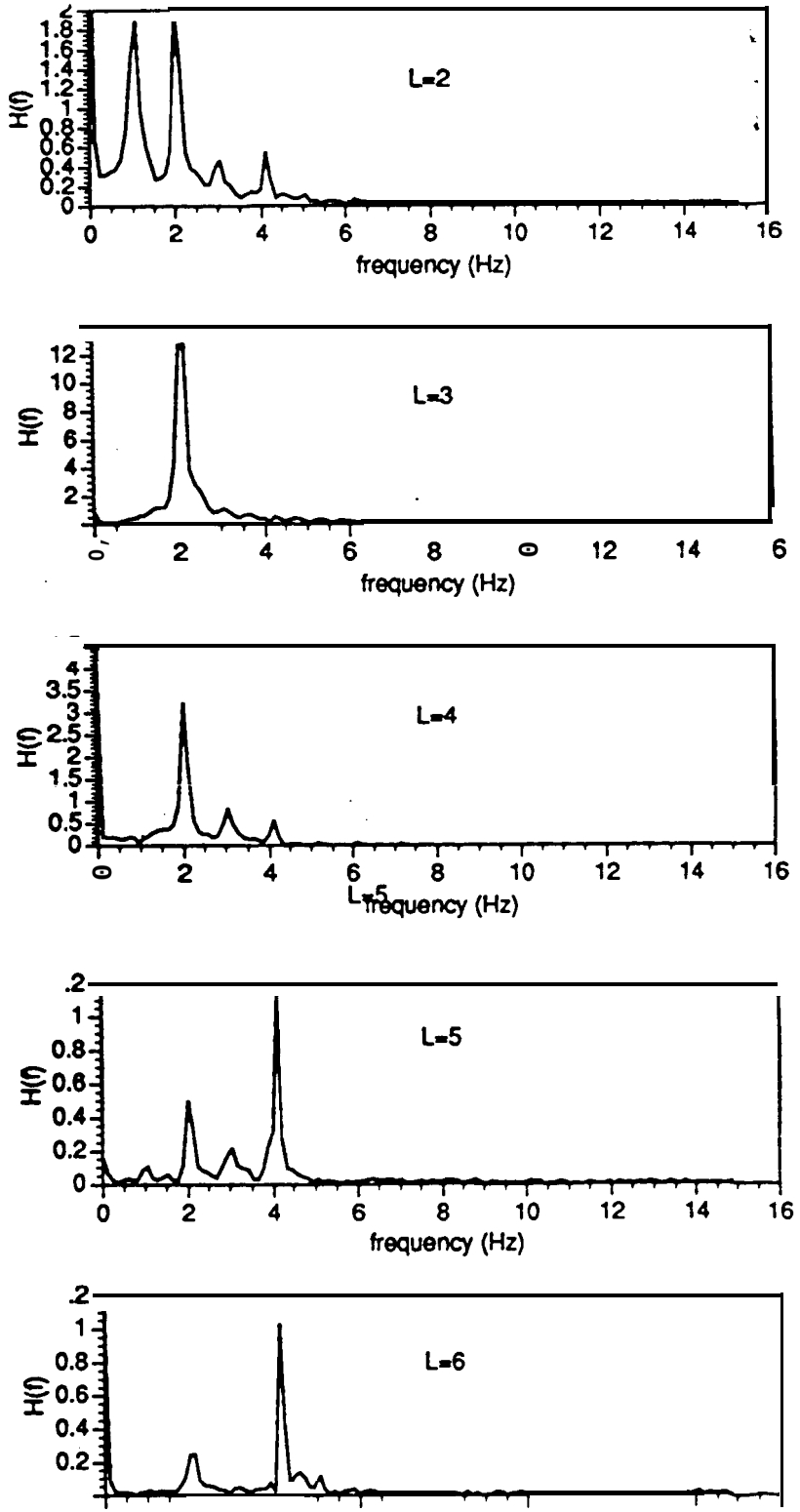

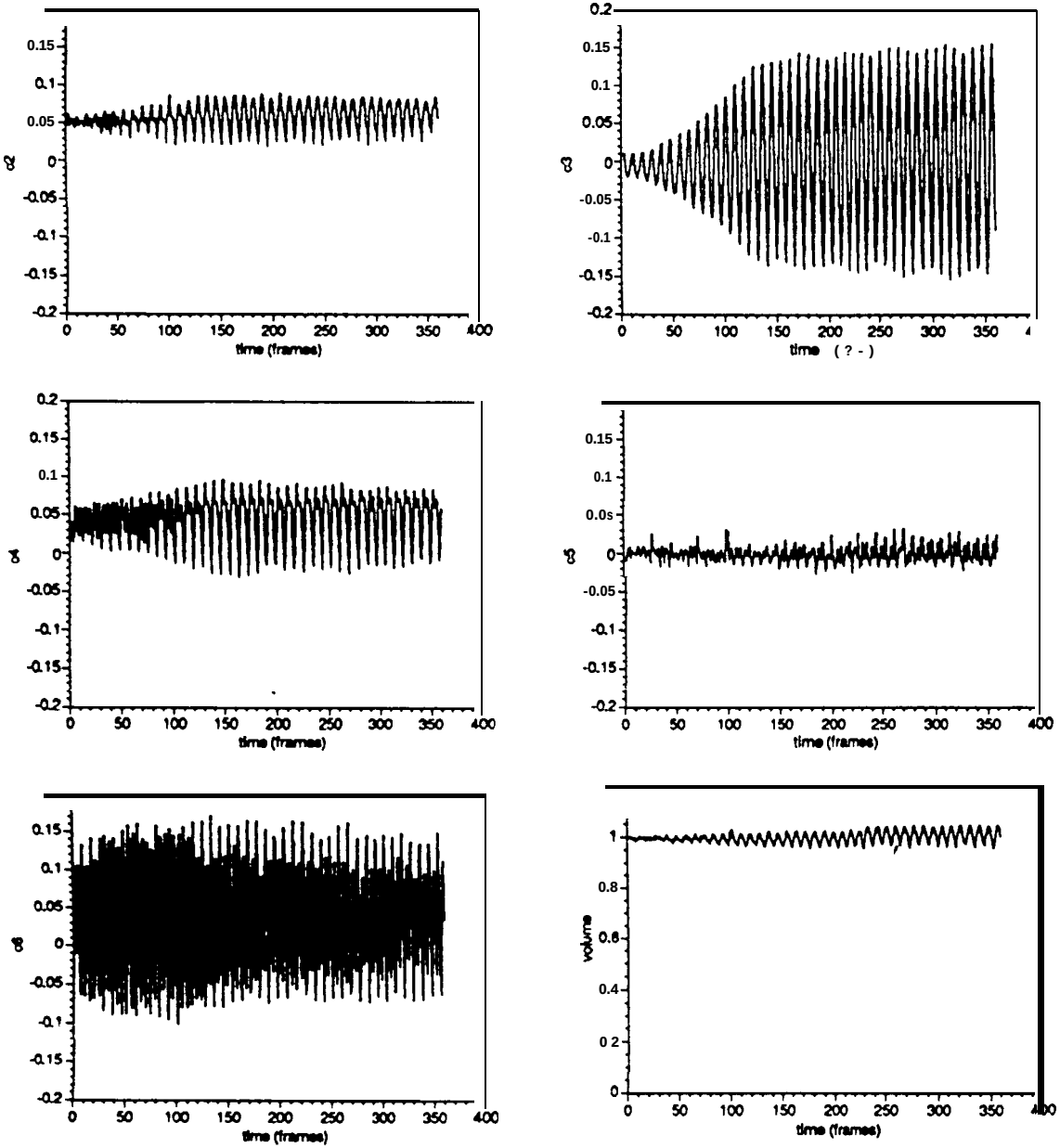

Fig. 7a

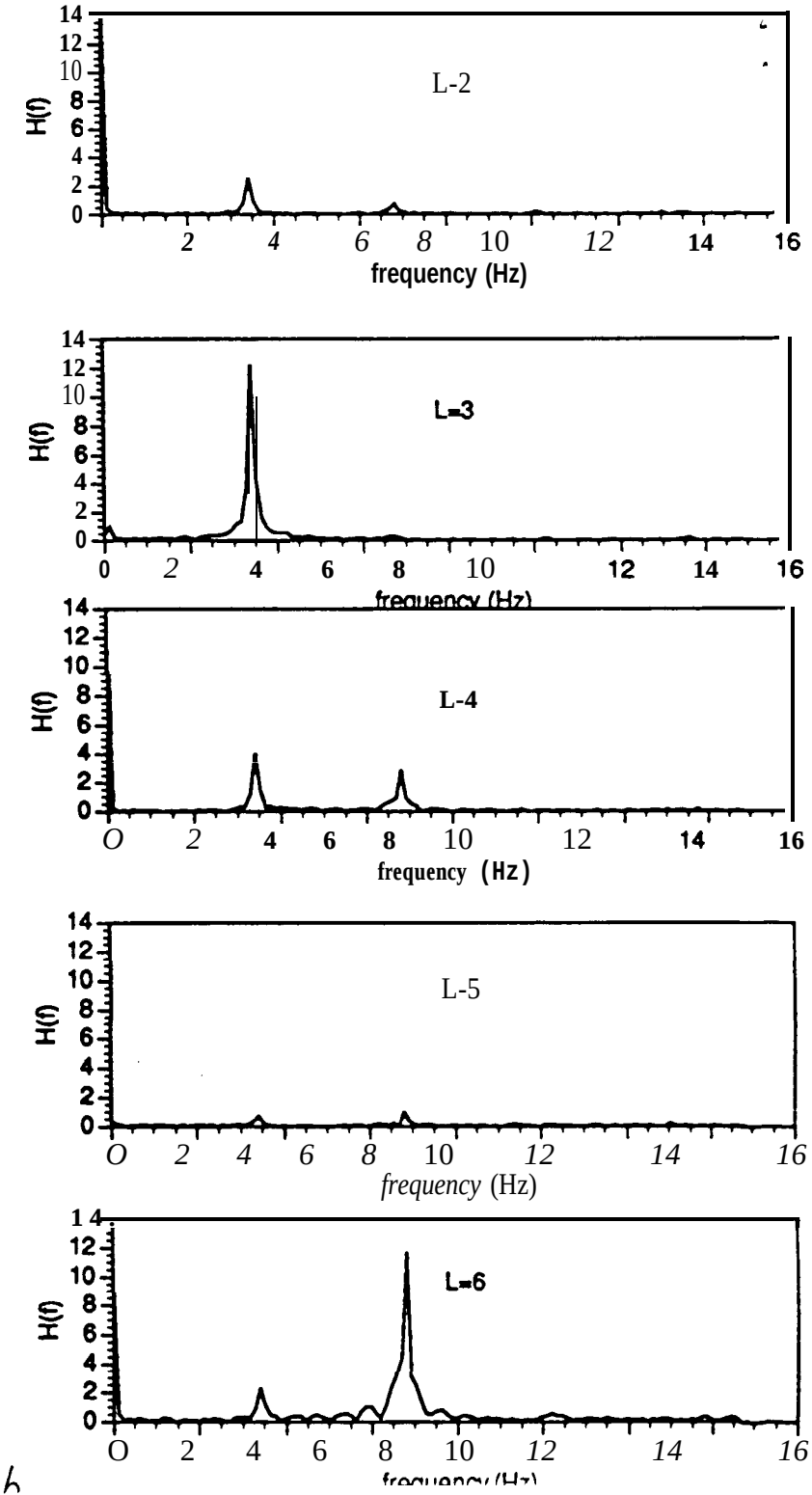

Fig. 7b

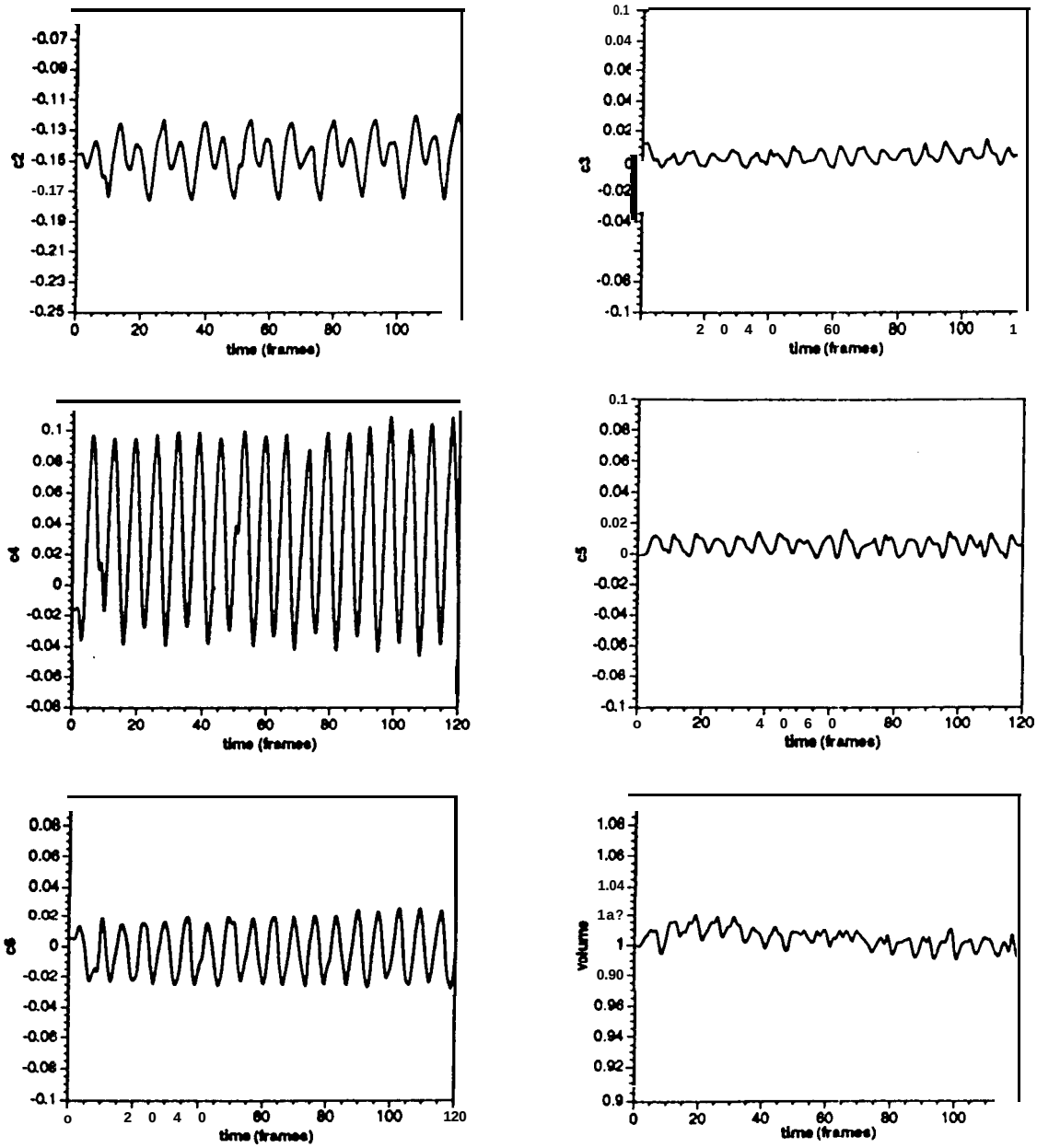
c2
time (frames)
c3
time (frames)
c4
time (frames)
c5
time (frames)
c6
time (frames)
volume
time (frames)

Fig. 8

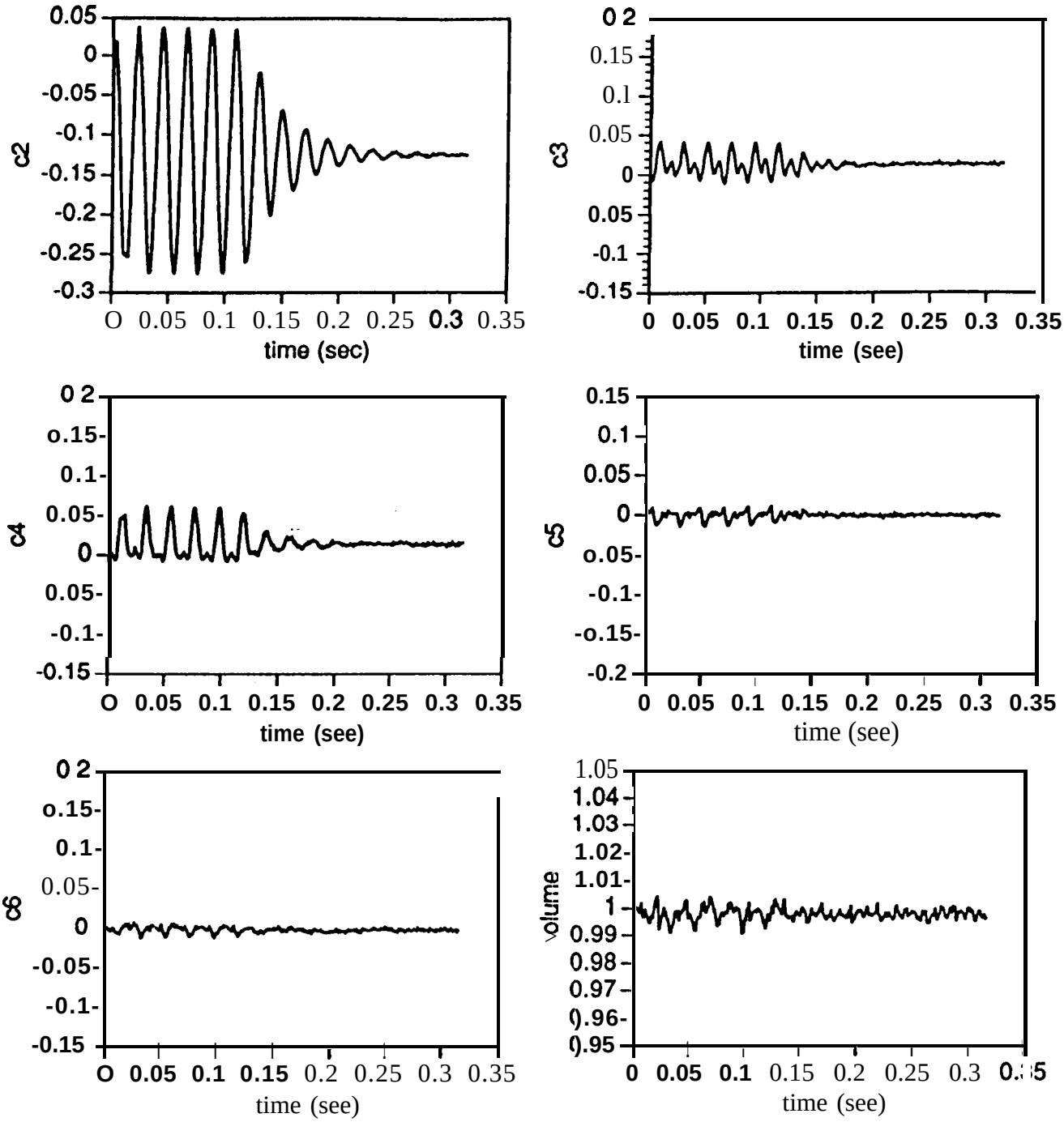
0.05
0
-0.05
-0.1
-0.15
-0.2
-0.25
-0.3
O 0.05 0.1 0.15 0.2 0.25 0.3 0.35
time (sec)
02
0.15
0.1
0.05
0
0.05
-0.1
-0.15
0 0.05 0.1 0.15 0.2 0.25 0.3 0.35
time (see)
02
o.15
0.1
0.05
0
0.05
-0.1
-0.15
O 0.05 0.1 0.15 0.2 0.25 0.3 0.35
time (see)
0.15
0.1
0.05
0
o.05
-0.1
-o.15
-0.2
0 0.05 0.1 0.15 0.2 0.25 0.3 0.35
time (see)
02
o.15
0.1
0.05
0
-0.05
-0.1
-0.15
O 0.05 0.1 0.15 0.2 0.25 0.3 0.35
time (see)
1.05
1.04
1.03
1.02
1.01
1
0.99
0.98
0.97
0.96
0.95
0 0.05 0.1 0.15 0.2 0.25 0.3 0.35
time (see)

Fig. 9

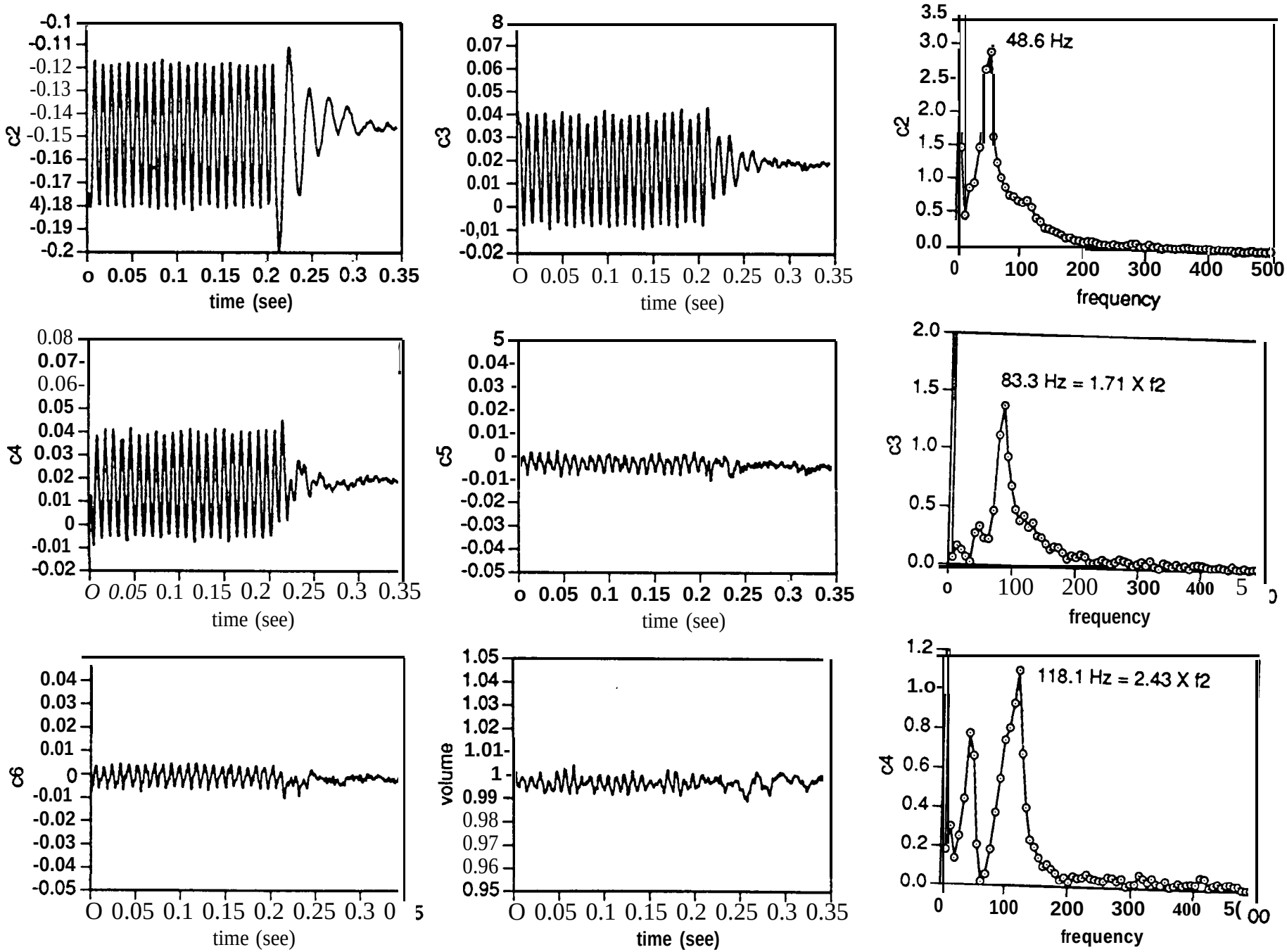
c2
time (see)
c3
time (see)
48.6 Hz
frequency
c4
time (see)
c5
time (see)
83.3 Hz = 1.71 X f2
frequency
c6
time (see)
volume
time (see)
118.1 Hz = 2.43 X f2
frequency

Fig 10

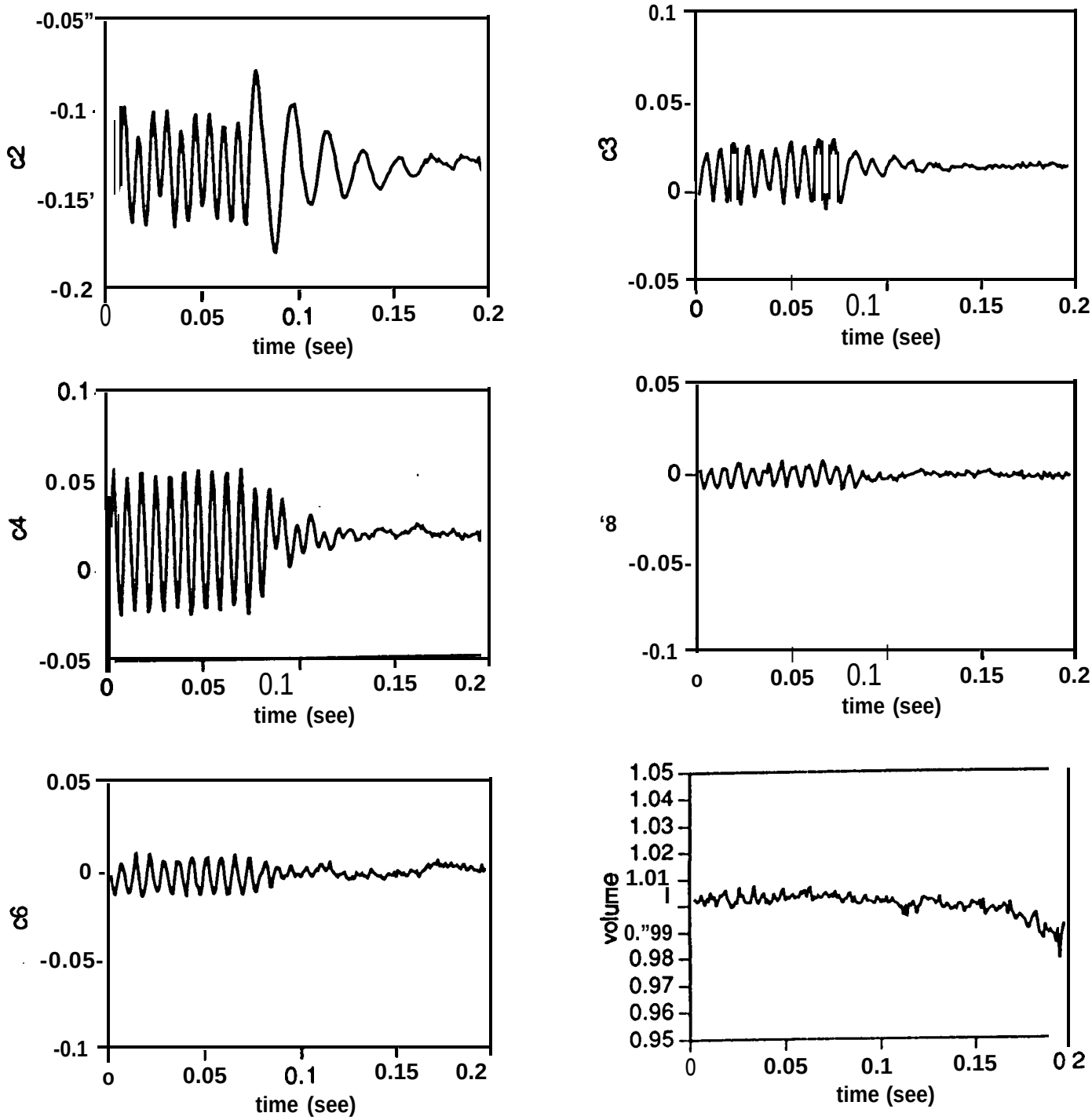
-0.05"
-0.1
-0.15'
-0.2
c2
0
0.05
0.1
0.15
0.2
time (see)
0.1
0.05
0
-0.05
c3
0
0.05
0.1
0.15
0.2
time (see)
0.1
0.05
0
-0.05
c4
0
0.05
0.1
0.15
0.2
time (see)
0.05
0
-0.05
-0.1
'8
o
0.05
0.1
0.15
0.2
time (see)
0.05
0
-0.05-
-0.1
c6
o
0.05
0.1
0.15
0.2
time (see)
1.05
1.04
1.03
1.02
1.01
0."99
0.98
0.97
0.96
0.95
volume
0
0.05
0.1
0.15
0 2
time (see)

Fig. 11